



Published in final edited form as:

Biomaterials. 2015 December ; 73: 120–130. doi:10.1016/j.biomaterials.2015.09.021.

Inhibition of osteoblast mineralization by phosphorylated phage-derived apatite-specific peptide

Janani Ramaswamy^a, Hwa Kyung Nam^b, Harsha Ramaraju^a, Nan E. Hatch^b, and David H. Kohn^{a,c,*}

Janani Ramaswamy: jananir@umich.edu; Hwa Kyung Nam: hknam@umich.edu; Harsha Ramaraju: sramara@umich.edu; Nan E. Hatch: nhatch@umich.edu; David H. Kohn: dhkohn@umich.edu

^aDepartment of Biomedical Engineering, University of Michigan, Ann Arbor, MI

^bDepartment of Orthodontics and Pediatric Dentistry, University of Michigan, Ann Arbor, MI

^cDepartment of Biologic & Materials Sciences, University of Michigan, Ann Arbor, MI

Abstract

Functionalization of biomaterials with material- and cell-specific peptide sequences allows for better control of their surface properties and communication with the surrounding environment. Using a combinatorial phage display approach, we previously identified the peptide VTKHLNQISQSY (VTK) with specific affinity to biomimetic apatite. Phosphorylation of the serine residues of the peptide (pVTK) caused a significant increase in binding to apatite, as well as a dose-dependent inhibition of osteoblast mineralization. In this study, we investigated the mechanisms behind pVTK mediated inhibition of mineralization using MC3T3 cells and testing the hypothesis that mineralization is inhibited via alteration of the Enpp1-TNAP-Ank axis. Inhibition of mineralization was not due to disruption of collagen deposition or calcium chelation by the negatively charged pVTK. The timing of peptide administration was important in inhibiting mineralization - pVTK had a greater effect at later stages of osteogenic differentiation (days 7–12 of culture corresponding to matrix maturation and mineralization), and could prevent progression of mineralization once it had started. pVTK treatment resulted in a significant decrease in ectonucleotide pyrophosphatase/phosphodiesterase 1 (Enpp1) enzyme activity and gene expression. The expression of ankylosis protein (Ank) and osteopontin (OPN) and Pit-1 genes was also significantly reduced with peptide treatment, while tissue non-specific alkaline phosphatase (TNAP), bone sialoprotein (BSP), and Runx2 gene expression was significantly higher. The ability of pVTK to inhibit mineralization can potentially be translated into therapeutics against pathological calcification seen in cardiovascular disease, osteoarthritis or craniosynostosis, or be used to prevent failure of biomaterials due to calcification, such as bioprosthetic heart valves.

*Corresponding author: 2213 School of Dentistry, 1011 North University Avenue, Ann Arbor, MI 48109-1078. Tel.: +1 734 764 2206; Fax: +1 734 647 2110.

Publisher's Disclaimer: This is a PDF file of an unedited manuscript that has been accepted for publication. As a service to our customers we are providing this early version of the manuscript. The manuscript will undergo copyediting, typesetting, and review of the resulting proof before it is published in its final citable form. Please note that during the production process errors may be discovered which could affect the content, and all legal disclaimers that apply to the journal pertain.

Keywords

Biominaleralisation; pathologic calcification; osteoblast; peptide; phage display

1. Introduction

Biomaterials should be able to communicate with their microenvironment, to encourage attachment of specific populations of cells onto their surfaces, and eventually regenerate functional tissue. Surface modification of biomaterials with cell-specific biological factors can provide the signals required to initiate cell adhesion. One approach to controlling biomaterial surface properties is via functionalization with cell- and material-specific peptide sequences, which can serve as anchors between a specific cell population and a specific material chemistry. Short synthetic peptides (9–30 amino acids in length) are advantageous for this application since they can be designed to be non-immunogenic, as well as more specific than full length proteins (containing multifunctional domains). Further, short peptides are easier and less expensive to synthesize, and are less likely to change conformation since they are not as prone to forming secondary/tertiary structures [1].

Peptide functionalized apatite-based biomaterials are useful in bone tissue engineering as they mimic aspects of the organic/inorganic hybrid composition of bone (primarily comprised of organic collagen and non-collagenous proteins, and inorganic hydroxyapatite). Traditionally, peptide sequences for bone regeneration have been derived from known bone-binding motifs found in non-collagenous proteins, often containing chains of acidic aspartate and glutamate residues. For example, the peptide EEEEEEEPRGDT (E7PRGDT), derived from bone sialoprotein (BSP), consists of a poly-glutamic hydroxyapatite binding domain and the ubiquitous RGD cell binding domain, and mediates osteoblast attachment to hydroxyapatite and subsequent osteogenesis [2,3]. The fusion peptide N15-PGRGDS, comprising a hydroxyapatite binding sequence (N15) derived from statherin and the RGD cell binding sequence from osteopontin (OPN), facilitates dose-dependent attachment of cells to hydroxyapatite [4]. Modular peptides have also been designed that contain apatite binding sequences derived from osteocalcin (OCN) and growth factor sequences derived from bone morphogenetic protein 2 (BMP2) [5]. These peptides modulate cell binding to apatite, and peptide-coated implants stimulate greater bone formation and ingrowth compared to untreated controls in a sheep bone-implant gap model [6].

A novel way of discovering unique material-specific peptides is through the use of phage display, which involves panning bacteriophage libraries expressing $\sim 10^9$ sequences against a material of interest. Using this approach, along with computational modeling and ELISA, we identified the apatite-specific 12-mer peptide VTKHLNQISQSY (VTK) [7,8]. However, a disadvantage of phage libraries is the inability of bacteriophage to incorporate peptide post translational modifications, such as phosphorylation of serine, threonine and tyrosine residues, which are particularly important in the regulation of biomineralization [9,10]. To overcome this drawback and further characterize the mineral-binding VTK sequence, we phosphorylated the serine residues on VTK (pVTK) and measured a 10-fold increase in adsorption to synthetic biomimetic apatite, and significantly higher binding affinity of pVTK compared to non-phosphorylated VTK [11].

Additionally, pVTK caused a dose dependent inhibition of mineralization in MC3T3 pre-osteoblastic cells, with minimal cytotoxic effects. Although VTK and pVTK bind to both synthetic and cell-secreted mineral, the relative contribution of peptide sequence and charge is different between the two forms of apatite. Phosphorylation and net charge were more important in peptide binding to synthetic mineral (scrambling the sequence had no effect on binding to biomimetic mineral), whereas peptide sequence and phosphorylation/charge were equally important in inhibiting biological mineralization (scrambling pVTK resulted in 30% less inhibition compared to pVTK) [11]. Understanding how the phosphorylated peptide interacts with mineral and/or cells to inhibit mineralization could enable the application of pVTK in the treatment of pathological mineralization.

Development of therapeutics against pathological calcification is dependent on advancing knowledge of mechanisms of mineralization. Briefly, mineralization is a tightly regulated process determined by the concentrations and properties (including net charge, charge distribution or number of acidic/phosphorylated amino acid residues) of extracellular matrix proteins and other promoter and inhibitor molecules. Inorganic extracellular pyrophosphate (PPi) is a natural inhibitor of mineralization (at micromolar concentrations) and is formed as a by-product of several metabolic reactions. The concentration of extracellular PPi is regulated mainly by the action of tissue non-specific alkaline phosphatase (TNAP), ectonucleotide pyrophosphatase/phosphodiesterase 1 (Enpp1) and the progressive ankylosis protein (Ank). Enpp1 and Ank help inhibit calcification by increasing the concentration of extracellular PPi – Enpp1 cleaves ATP to release PPi and Ank transports PPi from within to outside the cell [12,13]. TNAP decreases PPi levels by cleaving PPi to generate phosphate (Pi), thus promoting calcification [14,15]. The actions of TNAP, Enpp1 and Ank maintain the PPi/Pi ratio, which has a direct consequence on mineralization – high PPi/Pi ratios inhibit, while low PPi/Pi ratios promote mineralization. The presence of Enpp1, Ank, TNAP, as well as other osteogenic markers in pathologic mineral deposits [16,17], indicate similarities between physiological (bone) and pathological calcification mechanisms, providing new opportunities for development of therapeutics against pathological calcification.

In this study, we hypothesized that pVTK inhibits MC3T3 mineralization via alteration of the Enpp1-TNAP-Ank axis. We performed assays at the gene and protein-levels to test the effect of peptide treatment on mineralization, collagen deposition, Enpp1 and TNAP enzyme activity, and osteogenic differentiation in MC3T3 cells. The effect of peptide administration on mineralization at various stages of osteogenic differentiation, and the ability to inhibit progression of mineralization in cultures after the initiation of mineralization were also investigated.

2. Materials and Methods

2.1 Peptide synthesis

The following peptides were used: pVTK (VTKHLNQI(pS)Q(pS)Y; pS = phosphoserine), FITC-pVTK (FITC-VTKHLNQI(pS)Q(pS)Y) and FITC-E7-RGD (FITC-EEEEEEPRGDT). Peptides were synthesized using Fmoc solid-phase chemistry according to standard peptide synthesis procedures and characterized as having >90 % purity by high-

performance liquid chromatography (University of Michigan Proteomics & Peptide Synthesis Core). Phosphorylation at specific serine residues was achieved using preformed, protected phosphoserine amino acids. For experiments involving fluorescence, peptides were labelled on resin before cleavage using 5-(and-6)-carboxyfluorescein succinimidyl ester (Molecular Probes C-1311). The peptides were dissolved in ddH₂O and aliquots were frozen at -20°C until ready to use in experiments.

2.2 Cell culture and overview of experimental design

MC3T3-E1 (subclone 14) murine calvarial pre-osteoblasts were maintained in alpha minimum essential medium supplemented with 10% fetal bovine serum and 1% penicillin-streptomycin (growth medium) at 37°C and 5% CO₂ in a humidified incubator. For all experiments, cells were seeded at a density of 10,000 cells/cm² (48 well plates, Corning Costar) and allowed to attach overnight in growth medium. Cells were then differentiated with osteogenic medium (growth medium supplemented with 10mM β-glycerophosphate and 50µg/ml ascorbic acid) with or without 300µM pVTK peptide and cultured for up to 12 days. Media was replaced every 2 days. For analysis of calcium, media was collected every two days during the media change and frozen at -80°C until assayed.

To understand the effect of pVTK on differentiation and mineralization, gene expression of Enpp1, TNAP, Runx2, bone sialoprotein, osteocalcin, osteopontin, Ank and Pit-1 was measured at days 3, 7, 10 and 12. The expression of collagen I was also measured after 12 days of peptide treatment. Protein expression (Runx2, OPN) and enzyme activity (Enpp1, TNAP) were also measured to confirm the gene-level data. To further determine the inhibitory effects of the peptide at different stages of osteogenic differentiation and mineralization, cells were cultured for 12 days with pVTK added at days 1–6 only (corresponding to cell proliferation and matrix production) or days 6–12 only (corresponding to matrix maturation and mineralization), and compared to untreated controls and cells cultured with the peptide for the entire 12 days. To assess the effect of peptide on mineralizing cell layers, cells were cultured in osteogenic media only until mineralization started on day 10, after which pVTK was added and cells were cultured until day 14.

2.3 Enpp1 and TNAP enzyme activity assays

Cell layers were washed with PBS and harvested in a 10mM Tris-HCl, 2mM PMSF, 0.2% Igepal solution. Samples were frozen at -80°C until assayed, at which time they were thawed, homogenized on ice and centrifuged at 12,600 rpm for 10 min at 4°C. Supernatants were used to assay for TNAP and Enpp1 activities using substrates p-nitrophenyl phosphate (Sigma Aldrich) and thymidine 5' – monophosphate p-nitrophenyl ester sodium salt (Sigma Aldrich), respectively, and absorbance was measured at 405nm using a microplate reader. A standard curve was used to correlate absorbance units to enzyme concentration, and values were normalized to total protein content (obtained from BCA assays (Pierce) performed with cell lysate supernatants).

2.4 Detection and quantification of mineralization

von Kossa staining was used to visualize mineralization of cell layers. Briefly, cells were washed with PBS, fixed in zinc buffered formalin for 30 min and rehydrated using a series

of graduated ethanol-water mixes. Cells were then exposed to 5% silver nitrate for 30–60 min in bright light. Wells were washed, dried and imaged using a Canon dissecting microscope. Quantification of the area covered by mineral was performed using ImageJ software (NIH). To quantify inorganic calcium levels deposited in cell matrices, cell pellets (obtained from cell lysis and centrifugation described above) were demineralized in 0.6N HCl overnight and calcium content in the supernatants was determined colorimetrically using a Stanbio Total Calcium LiquiColor kit. Calcium content was quantified using a standard curve and normalized to total protein content (obtained from BCA assays (Pierce) performed with cell lysate supernatants). Calcium content in culture media was similarly determined.

2.5 Picrosirius Red collagen staining

Cell layers were washed with PBS and fixed in Bouin's fluid for 1h. After washing with water, cells were stained with Sirius Red dye for 1h on a shaker. A standard curve was created by pipetting known concentrations of calf skin collagen (Sigma Aldrich, dissolved in acetic acid) onto microtiter plates, followed by air drying and staining. To quantify the collagen content, wells were destained with 0.1N NaOH for 30 min, absorbance read at 550nm and the collagen content was determined from the standard curve.

2.6 Western Blots

Cell layers were harvested in lysis buffer containing 150mM NaCl, 50mM TrisCl, 1mM EDTA, 1% Triton, 1% sodium deoxycholate, 0.1% SDS and protein inhibitor cocktail (Cell Signaling) and frozen at -80°C . Samples were thawed, homogenized on ice and centrifuged at 12,600 rpm for 10 min at 4°C , and protein levels were quantified from the supernatants using the BCA assay (Pierce). 10ug or 25ug of protein (for osteopontin or Runx2 respectively) were mixed with Laemmli loading buffer, boiled and cooled, and separated using SDS-PAGE. Proteins were transferred onto PVDF membranes (Millipore) and blocked in 5% non-fat milk. Membranes were first probed with primary antibodies in 5% non-fat milk or bovine serum albumin and then with horse radish peroxidase (HRP)-conjugated secondary antibodies in 5% non-fat milk. Bands were visualized by chemiluminescence using SuperSignal West Pico substrate (Thermo Scientific). The following primary antibodies and dilutions were used: goat anti-osteopontin (AF808, R&D Systems) at 1:5000, mouse anti-Runx2 (D130-3, MBL International) at 1:500 and rabbit anti-GAPDH (14C10, Cell Signaling Technology) at 1:1000. The following HRP-conjugated secondary antibodies and dilutions were used: anti-goat (A8919, Sigma Aldrich) at 1:20000, anti-mouse (W402B, Promega) at 1:7500 and anti-rabbit (A0545 Sigma Aldrich) at 1:5000.

2.7 Quantitative Real Time PCR

Cells were washed with PBS, total RNA was extracted using TRIzol (Invitrogen) and cDNA was synthesized using Taqman cDNA synthesis kit (Applied Biosystems). Real Time PCR was performed using manufacturer protocols (Applied Biosystems) and mRNA levels measured using a standard curve. The following murine genes were measured using Taqman primer/probes: *Enpp1* Enpp1 (Mm01193752_m1), *Alpl* TNAP (Mm00475834_m1), *Ibsp*

BSP (Mm00492555_m1), *Bglap* OCN (Mm03413826_mH), *Ank* Ank (Mm00445050_m1), *Coll1a1* Col1 (Mm00801666_g1), *Runx2* Runx2 (Mm00501578_m1), *Slc20a1* Pit-1 (Mm00489378_m1) and normalized to the housekeeping gene *Hprt1* (Mm01545399_m1). Q-RT-PCR studies were repeated at least twice for the majority of genes measured in this study, using different batches of cells and mRNA, and PCR was run on different days to confirm reproducibility of the findings. Data is presented as averages of triplicate or quadruplicate samples from one of the repeated experiments. Peptide effects are shown as fold changes relative to osteogenic treatment without peptide.

2.8 Cell internalization of peptide

MC3T3 cells were seeded at a density of 15,000 cells/cm² on tissue culture treated glass coverslips in 24 well plates. Peptides were dissolved in ddH₂O and diluted to 300µM in OPTIMEM (Invitrogen). After media was removed, adherent cells were incubated with 300µM of FITC-pVTK, FITC-E7-RGD, and OPTIMEM control media (no peptide) for 1hr. Cells were subsequently washed in PBS, fixed in 10% neutral buffered formalin, and mounted on glass slides in Vectashield containing the nuclear stain DAPI (Vector Labs). Nikon Ti-Eclipse laser scanning confocal microscope was used to gather images (n=20 per group, across 4 samples). Each fluorescent channel, DAPI and FITC, was imaged individually and merged using Image J.

2.9 Statistics

Data is represented as mean ± one standard deviation. SigmaPlot was used to perform all statistical analyses. Sample sizes of n=3–4 per group were used in all experiments. One way ANOVA or ANOVA on Ranks with Student Neuman Keuls post hoc multiple comparisons tests were used to determine effect of treatment across time (i.e. within osteogenic media or osteogenic media containing peptide). t-tests or Mann Whitney Rank Sum tests were used to determine differences between treatments at specific time points or calcium concentrations. $p < 0.05$ denotes statistical significance.

3 Results

3.1 Effect of pVTK on mineralization and collagen matrix synthesis

Treatment of MC3T3 cultures with 300µM pVTK peptide for 12 days caused inhibition of mineralization compared to non-peptide treated controls cultured in osteogenic medium (Fig. 1A). To determine if inhibition of mineralization was caused by peptide disruption of collagen matrix deposition, cell layers were stained with PicroSirius Red. pVTK treatment did not inhibit collagen production; rather treatment with peptide resulted in significantly higher amounts of collagen compared to non-peptide controls cultured in osteogenic medium ($p = 0.044$; Fig. 1B). Similar trends of increased Col1 gene expression were seen with peptide treatment compared to osteogenic medium controls (Fig. 1C).

3.2 Effect of pVTK on different stages of cell differentiation

When peptide was added for the first 6 days of culture and then removed, cells were able to mineralize (Fig. 2). When cells were cultured without peptide from days 1–6 and peptide

added only for the last 6 days of culture, mineralization was significantly inhibited ($p < 0.05$).

3.3 Effect of pVTK on Enpp1 and TNAP

Enpp1 enzyme activity and gene expression were significantly inhibited with 12 days of peptide treatment (Fig. 3A, C; $p = 0.029$ vs. Osteo at both the enzyme and gene-levels). There was a trend of increased TNAP enzyme activity (Fig. 3B), while gene expression of TNAP was significantly higher with peptide treatment (Fig. 3D, $p < 0.001$ vs. Osteo).

3.4 Effect of pVTK on osteogenic gene expression

Runx2 and BSP levels were also significantly increased with 12 days of peptide treatment, whereas OPN, Pit-1 and Ank were significantly decreased compared to osteogenic medium controls (Fig. 4, Osteo + Peptide vs. Osteo for Runx2: $p = 0.009$, BSP: $p = 0.004$, OPN and Ank: $p = 0.029$, Pit-1: $p = 0.003$). There was no significant effect of peptide treatment on OCN.

3.5 Effect of pVTK on time course of osteogenic expression

To determine the specific times/stages at which the peptide affected osteogenesis and mineralization, gene expression was studied at days 3, 7 and 10 of culture (Fig. 5). Peptide treatment resulted in significantly lower Runx2 expression at day 3 ($p = 0.003$), but significantly higher expression at day 10 ($p = 0.029$ vs. Osteo). There was no significant effect of peptide treatment on BSP and TNAP, but a trend of higher expression in peptide treated samples on day 10. Significantly lower expression of OPN and Pit-1, and a trend of lowered expression of Enpp1 and Ank were observed with 10 days of peptide treatment (Osteo + Peptide vs. Osteo for OPN: $p = 0.002$; Pit-1: $p = 0.039$). Similar trends were seen in Runx2 and OPN protein expression; peptide treatment increased Runx2 expression at day 10 and decreased OPN expression at days 10 and 12 (Fig. 6). Overall, expression levels of genes involved in promoting mineralization (TNAP, Runx2, BSP, OCN) plateaued or declined by d10, whereas genes that inhibit mineralization (Enpp1, Ank, OPN) don't increase until d7–10. Moreover, this latter set of genes do not increase with pVTK. Peptide treatment resulted in a greater reduction (vs. Osteo) in the expression of the inhibitors OPN and Ank compared to the increases in expression of the promoters Runx2 and BSP (vs. Osteo).

3.6 Effect of pVTK addition to mineralized cell layers

From a clinical standpoint, it is important to be able to stop the progress of mineralization once it has started. To test if the phosphopeptide was able to stop mineralization after it had initiated, cells were cultured in osteogenic medium until they started to mineralize (by day 10), and peptide was then added for the remaining culture period until day 14. pVTK treatment significantly inhibited the progression of mineralization compared to untreated osteogenic media controls at day 12 (Fig. 7B, ~ 50% lower, $p = 0.003$ vs. Osteo), and also prevented further increases in mineralization from day 12 to day 14 (Fig. 7B, Osteo + Peptide: day 12 vs. day 14 not significant; day 14 Osteo vs. day 14 Osteo + Peptide $p = 0.006$). Enpp1 enzyme activity was also significantly decreased with peptide treatment at

day 12 (Fig. 7C, $p < 0.001$ vs. Osteo), while TNAP enzyme activity was significantly higher at day 14 (Fig. 7D, $p = 0.029$ vs. Osteo), compared to osteogenic media controls.

3.7 Cell internalization of peptide

Both FITC-peptides pVTK and E7-RGD were internalized by MC3T3 cells after 1 hr of incubation (Fig. 8A). However there was more observable translocation of pVTK within MC3T3 cells compared to E7-RGD. The FITC-pVTK signal was co-localized with the cytoskeletal structure of the cells. Additionally, vesicular associations surrounding many cellular nuclei (Fig. 8B) were also observed, indicating additional intracellular processing of the translocated pVTK peptide. No FITC signal was detected in the no-peptide controls.

3.8 Effect of pVTK on calcium chelation

The pVTK peptide has two phosphorylated amino acids and a net negative charge, and hence it is possible for the peptide to sequester calcium in solution, preventing mineralization. To test if this is a mechanism of pVTK-mediated inhibition of mineralization, media was collected at 2 day intervals from cells cultured in the presence or absence of peptide and assayed for soluble calcium levels (Fig. 9A). For untreated cells cultured in osteogenic media, calcium levels in the media remained constant over time until mineralization started (~ day 10), after which the calcium levels significantly decreased (Osteo day 10, 12 vs. days 2, 4, 6 and 8, $p < 0.001$). In contrast, media calcium levels remained constant at all times in peptide treated groups and were significantly higher than in untreated osteogenic medium controls on days 10 ($p = 0.003$) and 12 ($p = 0.047$). To determine if mineralization could be achieved by adding supplemental calcium, 0.5 or 1mM additional calcium chloride was added to cells with or without the peptide, and calcium deposition levels measured from demineralized cell layers (Fig. 9B). Supplementing calcium concentrations in the media resulted in increased calcium deposition in osteogenic medium controls (Osteo 0 mM vs. Osteo 0.5 mM $p = 0.016$, Osteo 0 mM vs. Osteo 1mM $p = 0.003$), but mineralization was still inhibited in peptide treated groups, suggesting that inhibition of mineralization is not due to sequestration of calcium.

4. Discussion

Deposition of minerals in soft tissues or the hypermineralization of bones occurs in a number of diseases, yet remains poorly understood. Coronary artery calcification is a strong predictor of cardiovascular mortality and coronary heart disease, which was responsible for approximately 1 in every 6 deaths in the United States in 2007 [18,19]. Craniosynostosis occurs at a frequency of 1 in 2500 live births and, if uncorrected, can cause craniofacial defects, retardation of brain development and death. However, despite the widespread prevalence and morbidity of these and other diseases resulting from pathological calcification, treatment options are often limited to surgery and/or drugs, and are characterized by inconsistent results, adverse side effects on other tissues, and a lack of clear knowledge on mechanisms. The data reported in this paper demonstrate the ability of a novel peptide, pVTK, to inhibit cellular mineralization *in-vitro* and a potential role for peptides in treating abnormal mineralization conditions *in-vivo*.

Phosphorylation of serine residues is an important post-translational modification via which mineralization is controlled. For example, the acidic and phosphorylated protein osteopontin loses its mineral inhibition potential when dephosphorylated [20,21]. Similarly, only the phosphorylated form of the VTK peptide (pVTK) inhibits mineralization of MC3T3 cells [11]. Mineralization can be disrupted or delayed by insufficient or aberrant collagen matrix deposition. However, pVTK treatment significantly increased collagen deposition (Fig. 1B) and Col1 gene expression (Fig. 1C) in MC3T3 cells. Further, in cells treated with peptide at early stages of culture (days 1–6 only), matrix mineralization was rescued once normal osteogenic culture conditions resumed at later stages of culture (days 7–12) (Fig. 2), suggesting the organic matrix, which serves as a template for mineralization, was not compromised by pVTK. Collectively, this data indicates that the inhibition of mineralization does not appear to be due to the peptide interfering with collagen deposition.

Clinically, pathological calcification is detected only after significant sized mineral deposits have formed, typically due to presentation of other related symptoms or because of limitations in detection resolution. However, once detected, it is important to be able to stop further progression of mineralization. To test the potential for inhibiting progression of mineralization, peptide was added to MC3T3 cultures that had already started to mineralize. pVTK significantly inhibited further mineralization (Fig. 7B) compared to osteogenic medium controls. This data is crucial to the application of the peptide to treat pathological calcification by stopping the progression of mineralization after it has started.

The pVTK peptide has two phosphorylated serine residues and consequently a net negative charge. These negatively charged groups can chelate positively charged calcium ions in solution and prevent mineralization. pVTK treatment resulted in significantly higher media calcium levels compared to non-treated controls starting at day 10, when the osteogenic controls started to mineralize and deplete the media of Ca (Fig. 9A). However, further supplementation of the medium with CaCl₂, which would compensate for any ion sequestration, did not result in mineralization (Fig. 9B), indicating that peptide-calcium sequestration is likely not a mechanism of mineralization inhibition.

The presence of osteochondrogenic markers in pathological mineral deposits and the role of these markers in the progression of pathological calcification indicate similarities in mechanisms between normal bone mineralization and abnormal calcification of soft tissue. For instance, bovine aortic smooth muscle cells mineralize under calcifying conditions, accompanied by loss of smooth muscle specific markers and upregulation of osteogenic markers [16]. Enpp1 knockout mice have widespread calcification of the coronary artery, aorta, kidneys and joints [17]. Hence, a better understanding of physiologic mineralization and the effect of anti-calcification drugs on mechanisms of mineralization will provide useful information in targeting and treating pathological calcification. In this paper, we studied the effect of pVTK peptide treatment on important regulators of osteoblast mineralization. Enpp1 and TNAP directly affect the PPi/Pi balance and play critical roles in the regulation of mineralization, along with other osteogenic markers, including OPN and BSP. Peptide treatment inhibited Enpp1 starting between day 7 and 10 of culture and this inhibition was sustained until the end of culture (Figs. 3, 5). The primary role of Enpp1 in osteoblasts is to break down nucleoside triphosphates, such as ATP, to generate PPi, a

natural inhibitor of mineralization [12]. Significant decreases were also seen in the expression of OPN and Ank after 10 – 12 days of treatment (Fig. 4, 5). Ank is a membrane transporter protein, responsible for transferring PPi from inside the cell to the extracellular environment [13]. OPN is a negatively charged and highly phosphorylated non-collagenous protein that prevents apatite nucleation and growth [9,22]. Expression of TNAP, Runx2 and BSP was significantly higher with pVTK peptide treatment for 10 – 12 days, compared to non-peptide treated controls cultured in osteogenic medium (Figs. 3, 4, 5). TNAP promotes mineralization by cleaving PPi (or β -glycerophosphate *in-vitro*) to generate Pi [14,15], whereas BSP acts as a nucleator of apatite [23]. Runx2 is an osteoblastic transcription factor and its overexpression enhances mineralization [24].

Collectively, our data show that Enpp1, OPN and Ank, which inhibit mineralization (directly or indirectly via PPi), were all significantly lowered with pVTK administration, whereas TNAP, Runx2 and BSP, which are positive regulators of mineralization, were all significantly increased with pVTK treatment. The gene expression data was also confirmed at the protein-level (Figs. 3 and 6). Since this scenario of gene and protein expression might be expected to increase mineralization, our findings of mineral inhibition suggest a possible compensatory mechanism where the peptide treated cells are attempting to rescue the reduced mineralization by downregulating the inhibitors and simultaneously upregulating the promoters (Fig. 10).

pVTK peptide was internalized by MC3T3 cells and localized to cytoskeletal and vesicular structures (Fig. 8). However, despite being taken up intracellularly within one hour of incubation, no effect of the peptide treatment was observed at early stages of culture, and most differences in gene and protein expression between peptide treated cells and controls occurred only after mineralization started (around day 10 of culture; Figs. 2 – 6). Additionally, pVTK binds strongly to both biomimetic synthetic mineral and MC3T3 secreted mineral, and computational modeling shows that the phosphoserine residues contribute most to apatite binding [11]. Hence, it is possible that the peptide inhibits mineralization via a combination of physico-chemical and cellular mechanisms, by binding strongly to the initially formed mineral nuclei and preventing further crystal growth. In response to this lack of mineralization and also by direct interaction with pVTK, the cells could be attempting to alter their gene expression towards a more pro-mineralization state (Fig. 10). Further investigation is necessary to characterize peptide-mineral interactions as well as determine specific cellular compartments involved in peptide internalization.

Measurement of intracellular and extracellular concentrations of Pi and PPi will also provide a better understanding of the effect of peptide on mineralization. In addition to their roles in hydroxyapatite formation, Pi and PPi also act as signaling molecules and directly affect osteogenic gene expression. Pi increases OPN and Pit-1 expression in MC3T3 cells [25,26]; PPi increases TNAP, OPN and Ank expression and also has a concentration-dependent effect on Enpp1 expression in MC3T3 cells [27]. pVTK caused an increase in TNAP and a decrease in Enpp1 and Ank expression (Figs. 3 – 5). Based on this expression profile, we would expect to find higher concentrations of extracellular Pi and lowered concentration of extracellular PPi, indicating a shift towards a pro-mineralization state with pVTK administration. However, we also observed lowered expression of Pit-1, a sodium-dependent

Pi transporter, which indicates potentially lowered intracellular concentrations of Pi. Pi needs to enter the cell to promote mineralization and influence changes in osteogenic gene expression [25,28,26]. Hence it is possible that lower intracellular Pi levels are also contributing to the lack of mineralization seen in response to peptide treatment, despite a gene expression profile favoring mineralization.

5. Conclusions

Phage-derived phosphopeptide pVTK was shown to inhibit mineralization and this inhibition was not due to disruption of collagen deposition or calcium chelation by negatively charged pVTK. The timing of peptide administration was important in inhibiting mineralization – pVTK treatment at later stages of differentiation (days 7–12) was more important in inhibiting mineralization. Further, this peptide could prevent progression of mineralization once it has started. pVTK also decreased the expression of Enpp1, Ank, OPN and Pit-1, while upregulating the expression of TNAP, BSP, OCN, Col1 and Runx2 in MC3T3 cells after 10 – 12 days of treatment. The ability of pVTK to inhibit mineralization can potentially be translated into therapeutics against pathological calcification seen in cardiovascular disease, osteoarthritis or craniosynostosis, or be used to prevent failure of biomaterials due to calcification, such as bioprosthetic heart valves.

Acknowledgments

The authors would like to acknowledge Dr. Henriette Remmer, Peptide Core for assistance with peptide synthesis and Taocong Jin, Molecular Biology Core for assistance with Q-RT-PCR. This work was supported by the National Institutes of Health: NIH DE 013380 and DE 015411 to DHK, JR, and HR, and OVPR grant to HKN and NEH. JR was the recipient of a Rackham Predoctoral Fellowship (2013–2014) from the University of Michigan Ann Arbor.

References

1. Hersel U, Dahmen C, Kessler H. RGD modified polymers: biomaterials for stimulated cell adhesion and beyond. *Biomaterials*. 2003; 24:4385–415. [PubMed: 12922151]
2. Fujisawa R, Wada Y, Nodasak Y, Kuboki Y. Acidic amino acid-rich sequences as binding sites of osteonectin to hydroxyapatite crystals. *Biochim Biophys Acta*. 1996; 1292:53–60. [PubMed: 8547349]
3. Fujisawa R, Mizuno M, Nodasaka Y, Kuboki Y. Attachment of Osteoblastic Cells to Hydroxyapatite by a Synthetic Peptide (Glu7-Pro-Arg-Gly-Asp-Thr) Containing Two Functional Sequences of Bone Sialoprotein. *Matrix Biol*. 1997; 16:21–8. [PubMed: 9181551]
4. Gilbert M, Shaw WJ, Long JR, Nelson K, Drobný GP, Giachelli CM, et al. Chimeric peptides of statherin and osteopontin that bind hydroxyapatite and mediate cell adhesion. *J Biol Chem*. 2000; 275:16213–8. [PubMed: 10748043]
5. Lee JS, Lee JS, Murphy WL. Modular peptides promote human mesenchymal stem cell differentiation on biomaterial surfaces. *Acta Biomater*. 2010; 6:21–8. [PubMed: 19665062]
6. Lu Y, Lee JS, Nemke B, Graf BK, Royalty K, Illgen R, et al. Coating with a modular bone morphogenetic peptide promotes healing of a bone-implant gap in an ovine model. *PLoS One*. 2012; 7:e50378. [PubMed: 23185610]
7. Segvich S, Biswas S, Becker U, Kohn DH. Identification of Peptides with Targeted Adhesion to Bone-Like Mineral via Phage Display and Computational Modeling. *Cells Tissues Organs*. 2008; 189:245–51. [PubMed: 18701808]
8. Segvich SJ, Smith HC, Kohn DH. The adsorption of preferential binding peptides to apatite-based materials. *Biomaterials*. 2009; 30:1287–98. [PubMed: 19095299]

9. Goldberg HA, Hunter GK. The Inhibitory Activity of Osteopontin on Hydroxyapatite Formation In Vitro. *Ann N Y Acad Sci.* 1995; 760:305–8. [PubMed: 7785906]
10. Addison W, Masica D, Gray J, McKee MD. Phosphorylation-Dependent Inhibition of Mineralization by Osteopontin ASARM Peptides is Regulated by PHEX Cleavage. *J Bone Miner Res.* 2009; 25:695–705. [PubMed: 19775205]
11. Addison WN, Miller SJ, Ramaswamy J, Mansouri A, Kohn DH, McKee MD. Phosphorylation-dependent mineral-type specificity for apatite-binding peptide sequences. *Biomaterials.* 2010; 31:9422–30. [PubMed: 20943264]
12. Terkeltaub R, Rosenbach M, Fong F, Goding J. Causal link between nucleotide pyrophosphohydrolase overactivity and increased intracellular inorganic pyrophosphate generation demonstrated by transfection of cultured fibroblasts and osteoblasts with plasma cell membrane glycoprotein-1. *Arthritis Rheum.* 1994; 37:934–41. [PubMed: 8003067]
13. Ho AM. Role of the Mouse ank Gene in Control of Tissue Calcification and Arthritis. *Science (80-).* 2000; 289:265–70.
14. Moss DW, Eaton RH, Smith JK, Whitby LG. Association of Inorganic-Pyrophosphatase Activity with Human Alkaline Phosphatase Preparations. *Biochem J.* 1967; 102:53–7. [PubMed: 6030299]
15. Hesse L, Johnson KA, Anderson HC, Narisawa S, Sali A, Goding JW. Tissue-nonspecific alkaline phosphatase and plasma cell membrane glycoprotein-1 are central antagonistic regulators of bone mineralization. *Proc Natl Acad Sci.* 2002; 99:9445–9. [PubMed: 12082181]
16. Steitz SA, Speer MY, Curinga G, Yang H-Y, Haynes P, Aebersold R, et al. Smooth Muscle Cell Phenotypic Transition Associated With Calcification: Upregulation of Cbfa1 and Downregulation of Smooth Muscle Lineage Markers. *Circ Res.* 2001; 89:1147–54. [PubMed: 11739279]
17. Mackenzie NCW, Zhu D, Milne EM, van 't Hof R, Martin A, Quarles DL, et al. Altered Bone Development and an Increase in FGF-23 Expression in Enpp1 Mice. *PLoS One.* 2012; 7:e32177. [PubMed: 22359666]
18. Vliegenthart R, Oudkerk M, Hofman A, Oei H-HS, van Dijck W, van Rooij FJa, et al. Coronary calcification improves cardiovascular risk prediction in the elderly. *Circulation.* 2005; 112:572–7. [PubMed: 16009800]
19. Roger VL, Go AS, Lloyd-Jones DM, Adams RJ, Berry JD, Brown TM, et al. Heart disease and stroke statistics--2011 update: a report from the American Heart Association. *Circulation.* 2011; 123:e18–209. [PubMed: 21160056]
20. Gericke A, Qin C, Spevak L, Fujimoto Y, Butler WT, Sørensen ES, et al. Importance of phosphorylation for osteopontin regulation of biomineralization. *Calcif Tissue Int.* 2005; 77:45–54. [PubMed: 16007483]
21. Jono S. Phosphorylation of Osteopontin Is Required for Inhibition of Vascular Smooth Muscle Cell Calcification. *J Biol Chem.* 2000; 275:20197–203. [PubMed: 10766759]
22. Boskey, aL; Maresca, M.; Ullrich, W.; Doty, SB.; Butler, WT.; Prince, CW. Osteopontin-hydroxyapatite interactions in vitro: inhibition of hydroxyapatite formation and growth in a gelatin-gel. *Bone Miner.* 1993; 22:147–59. [PubMed: 8251766]
23. Hunter GK, Goldberg HA. Nucleation of hydroxyapatite by bone sialoprotein. *Proc Natl Acad Sci.* 1993; 90:8562–5. [PubMed: 8397409]
24. Byers BA, García AJ. Exogenous Runx2 expression enhances in vitro osteoblastic differentiation and mineralization in primary bone marrow stromal cells. *Tissue Eng.* 2004; 10:1623–32. [PubMed: 15684671]
25. Beck GR, Zerler B, Moran E. Phosphate is a specific signal for induction of osteopontin gene expression. *Proc Natl Acad Sci U S A.* 2000; 97:8352–7. [PubMed: 10890885]
26. Beck G. Inorganic phosphate regulates multiple genes during osteoblast differentiation, including Nrf2. *Exp Cell Res.* 2003; 288:288–300. [PubMed: 12915120]
27. Addison WN, Azari F, Sørensen ES, Kaartinen MT, McKee MD. Pyrophosphate inhibits mineralization of osteoblast cultures by binding to mineral, up-regulating osteopontin, and inhibiting alkaline phosphatase activity. *J Biol Chem.* 2007; 282:15872–83. [PubMed: 17383965]
28. Beck GR. Inorganic phosphate as a signaling molecule in osteoblast differentiation. *J Cell Biochem.* 2003; 90:234–43. [PubMed: 14505340]

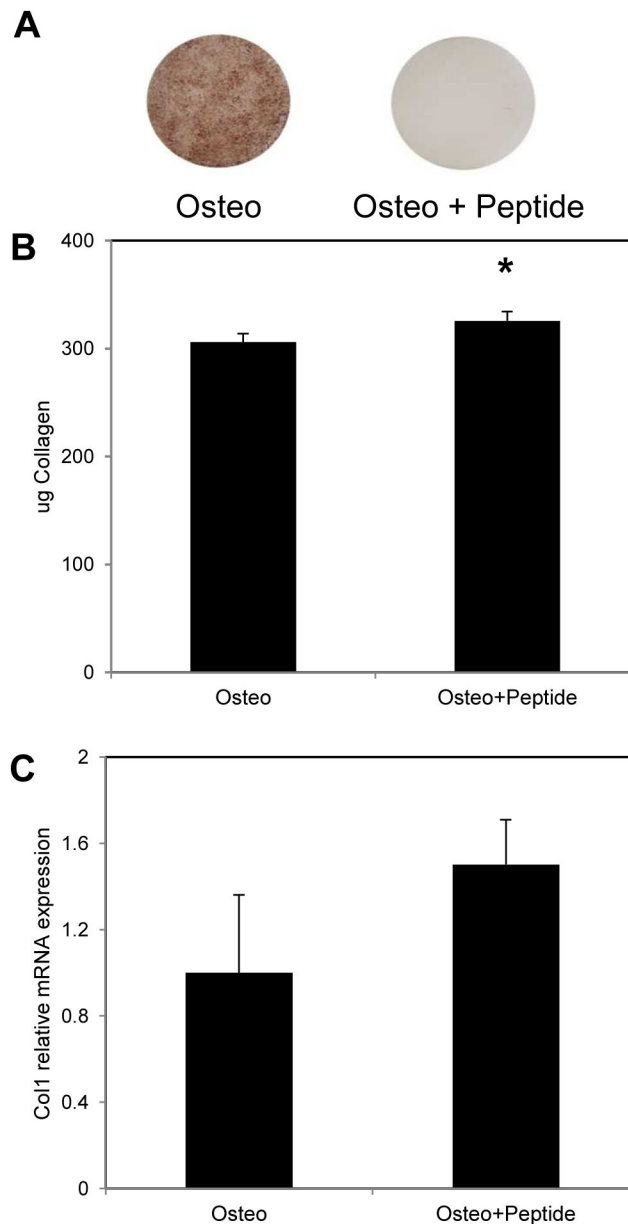


Figure 1. MC3T3 cells were cultured for 12 days in osteogenic (Osteo) or osteogenic medium supplemented with 300 μ M pVTK peptide (Osteo + Peptide) for 12 days. (A) von Kossa staining showed that peptide treatment inhibited mineralization compared to osteogenic medium controls; (B) Collagen quantification by PicroSirius Red staining showed that peptide treatment resulted in significantly higher collagen deposition compared to osteogenic medium; (C) Q-RT-PCR for Collagen (Col1) showed a trend of increased gene expression with peptide treatment relative to osteogenic treatment (normalized to Hprt housekeeping gene; * $p < 0.05$, t-test)

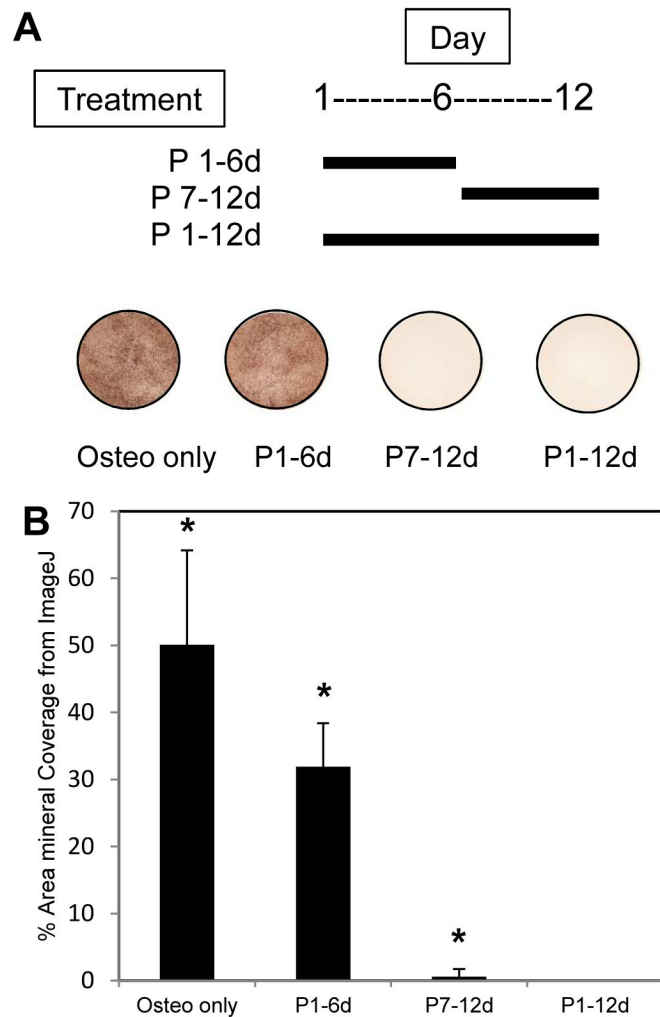


Figure 2.

MC3T3 cells were cultured for 12 days in osteogenic medium (Osteo) or osteogenic medium supplemented with 300 μ M pVTK peptide (Osteo + Peptide). Peptide was added during early stage culture (days 1–6 only, P1–6d), late stage culture (days 7–12 only, P7–12d) or all 12 days of culture (P1–12d). von Kossa staining and ImageJ analysis of percent area mineralized showed the lack of mineralization in cells treated with pVTK on days 7–12 only and for cells treated for all 12 days. Cells treated with peptide only on days 1–6 were still able to mineralize once peptide was removed. (* $p < 0.05$ compared to all other groups, 1 way ANOVA on Ranks, Student-Newman-Keuls post hoc test)

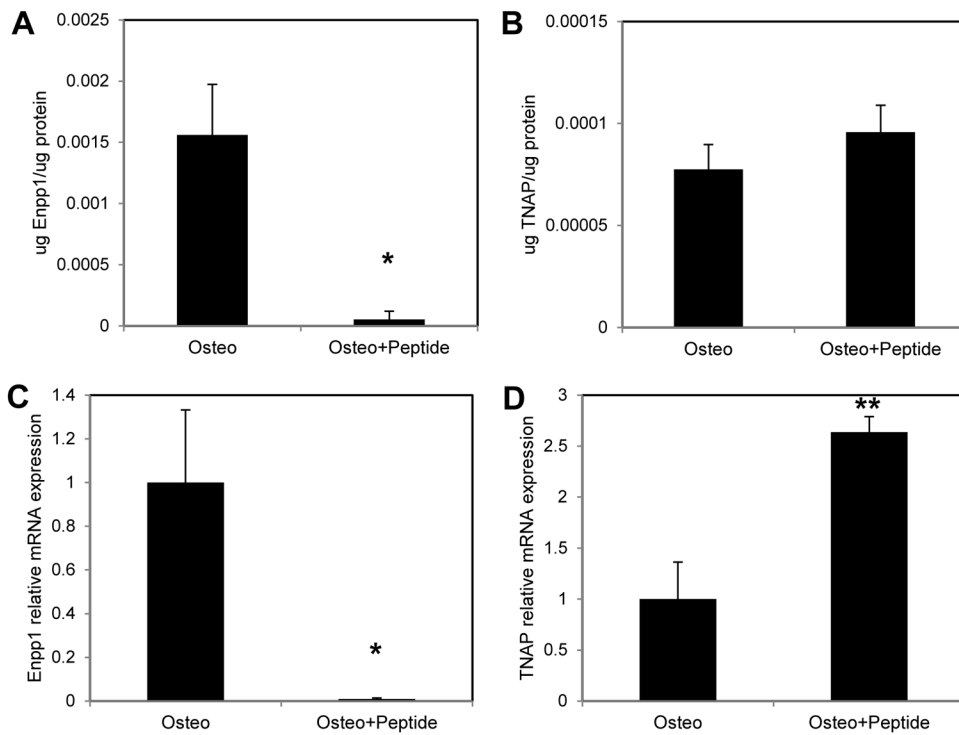


Figure 3.

MC3T3 cells were cultured in osteogenic medium (Osteo) or osteogenic medium supplemented with 300 μ M pVTK peptide (Osteo + Peptide) for 12 days. (A) Enpp1 enzyme activity was significantly inhibited with pVTK treatment compared to osteogenic medium; (B) TNAP enzyme activity was unaffected by pVTK treatment compared to osteogenic medium; (C) Q-RTPCR showed that gene expression of Enpp1 was significantly inhibited with peptide treatment relative to osteogenic medium; (D) Q-RTPCR showed that gene expression of TNAP was significantly increased with peptide treatment relative to osteogenic medium (normalized to Hprt; * $p < 0.05$, ** $p < 0.001$, t-test or Mann Whitney Rank Sum test)

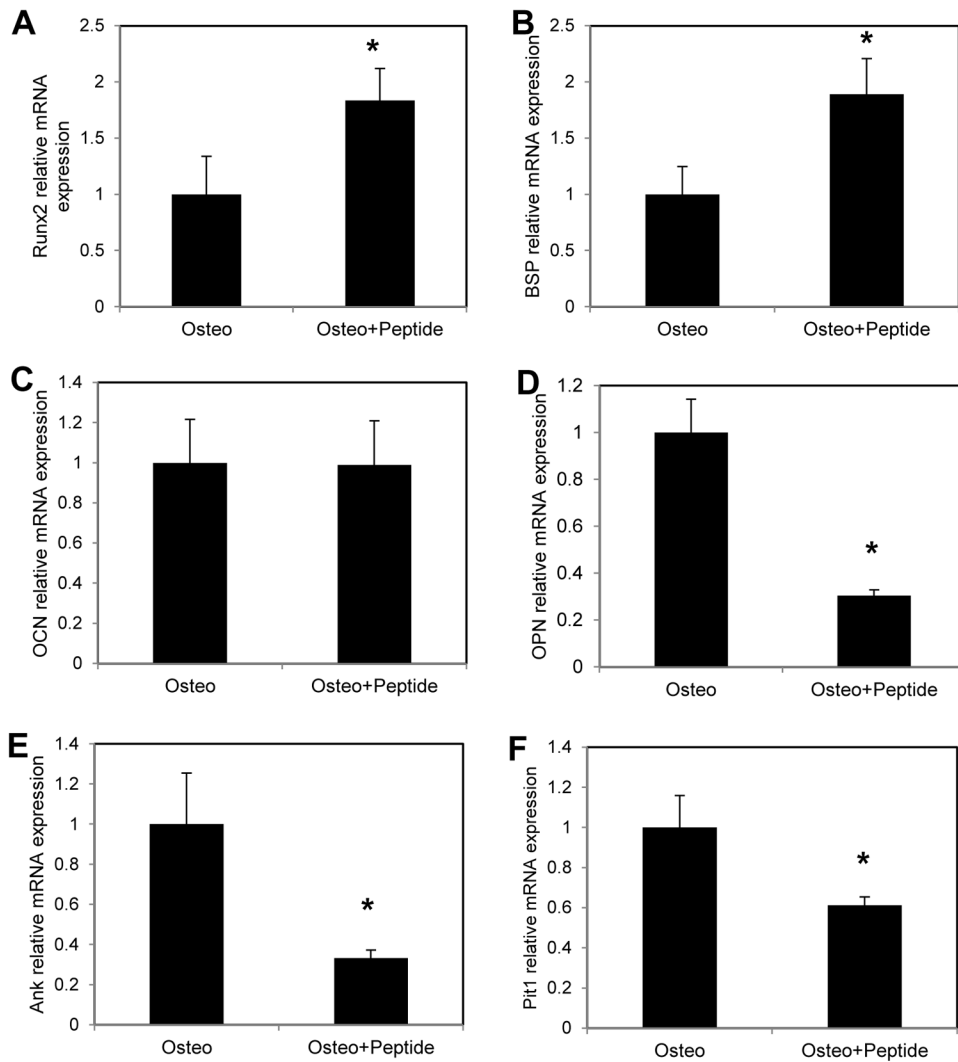


Figure 4.

MC3T3 cells were cultured in osteogenic medium (Osteo) or osteogenic medium supplemented with 300μM pVTK peptide (Osteo + Peptide) for 12 days. Q-RTPCR was used to measure gene expression of (A) Runx2, (B) BSP, (C) OCN, (D) OPN, (E) Ank and (F) Pit-1, all normalized to Hprt. Runx2 and BSP expression were significantly higher with pVTK treatment relative to osteogenic medium. OPN, Ank and Pit-1 expression was significantly lowered with pVTK treatment relative to osteogenic medium (normalized to Hprt housekeeping gene; * $p < 0.05$, t-test or Mann Whitney Rank Sum test)

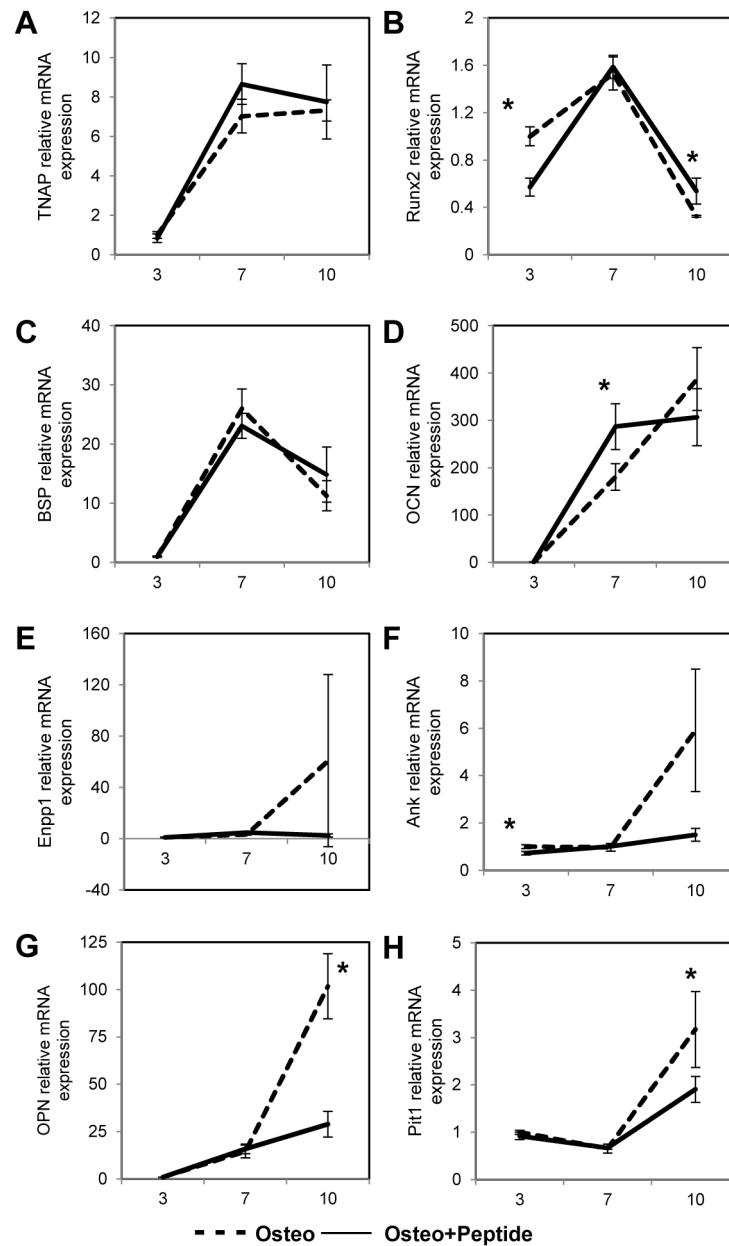


Figure 5.

MC3T3 cells were cultured in osteogenic medium (Osteo) or osteogenic medium supplemented with 300 μ M pVTK peptide (Osteo + Peptide) and gene expression of (A) TNAP, (B) Runx2, (C) BSP, (D) OCN, (E) Enpp1, (F) Ank, (G) OPN and (H) Pit-1, (all normalized to Hprt) was measured at days 3, 7 and 10 of culture via Q-RT-PCR. Peptide treatment resulted in significantly higher Runx2 expression at day 10 and a trend of higher expression of TNAP and BSP on day 10 relative to osteogenic medium. Significantly lowered expression of OPN and Pit-1, and a trend of lowered expression of Enpp1 and Ank were observed with 10 days of peptide treatment relative to osteogenic medium. (normalized to Hprt housekeeping gene; * p < 0.05, t-test or Mann Whitney Rank Sum test)

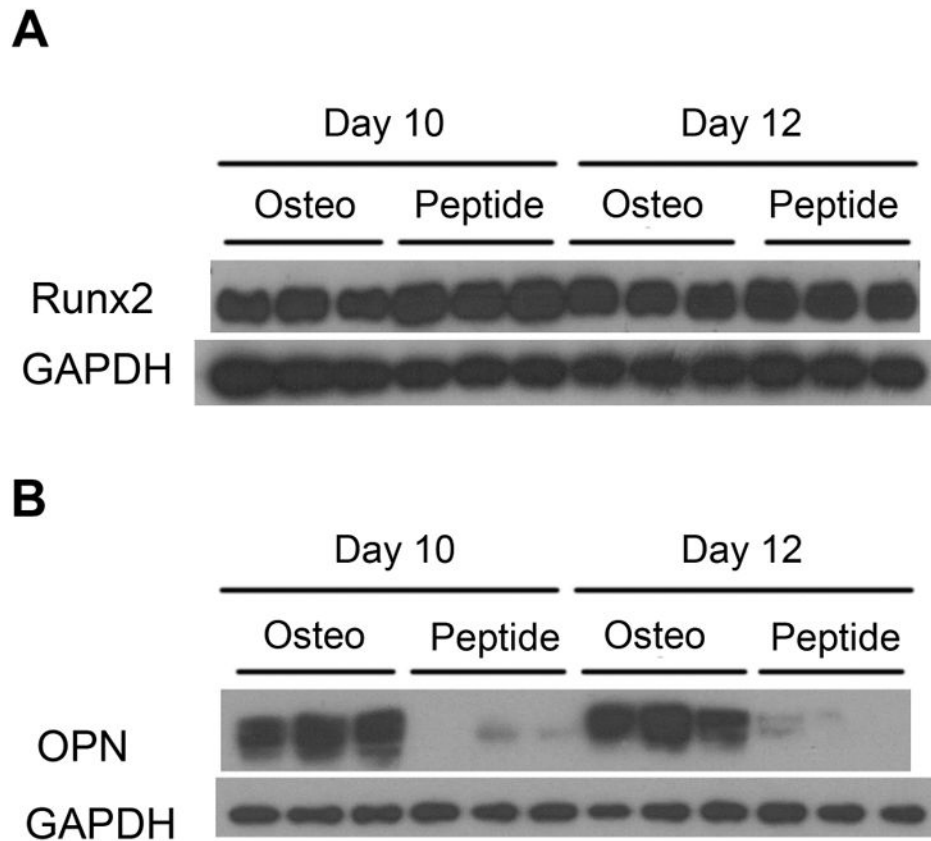


Figure 6.

MC3T3 cells were cultured in osteogenic medium (Osteo) or osteogenic medium supplemented with 300 μ M pVTK peptide (Osteo + Peptide) and protein expression of Runx2 and OPN was measured at days 10 and 12 of culture via Western Blotting. (A) Runx2 expression was increased at day 10 with peptide treatment vs. osteogenic medium; (B) OPN expression was decreased at days 10 and 12 with peptide treatment vs. osteogenic medium

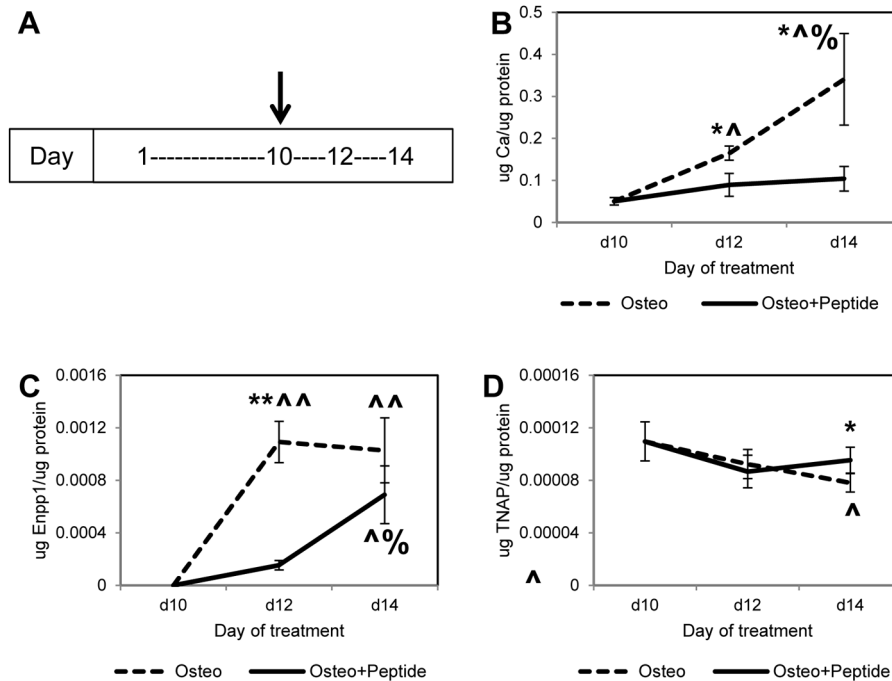


Figure 7.

MC3T3 cells were cultured for 10 days in osteogenic medium until mineralization started, at which time 300 μ M pVTK peptide was added (indicated by arrow on timeline (A)), and cultured for 4 additional days. (B) Calcium levels (quantified from demineralized matrices) and (C) Enpp1 enzyme activity were significantly reduced with peptide treatment (D) TNAP enzyme activity was significantly higher at day 14 with peptide treatment (* $p < 0.05$ Osteo vs. Osteo + Peptide at a specific day, t-test, ** $p < 0.001$ Osteo vs. Osteo + Peptide at a specific day, t-test, ^ $p < 0.05$ compared to day 10 within Osteo or Osteo + Peptide treatment group, ^^ $p < 0.001$ compared to day 10 within Osteo or Osteo + Peptide treatment group, % $p < 0.05$ compared to day 12 within Osteo or Osteo + Peptide treatment group, 1 way ANOVA or 1 way ANOVA on Ranks, Student-Newman-Keuls post hoc test)

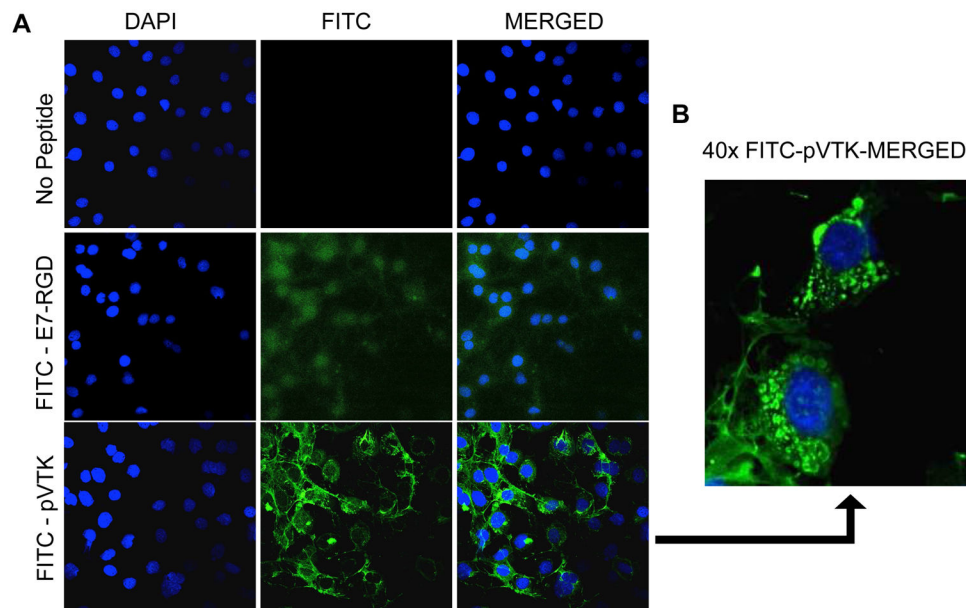


Figure 8. MC3T3 cells were incubated with or without FITC-tagged pVTK and E7-RGD peptides for 1 hour and their nuclei were stained with DAPI. Representative images of samples were obtained using scanning confocal microscopy and merged using Image J. (A) FITC-pVTK was associated with the cytoskeleton; 20X magnification (B) Magnified image of peptide-treated cells showed vesicular intracellular association of FITC-pVTK; 40X magnification scale bar 100um

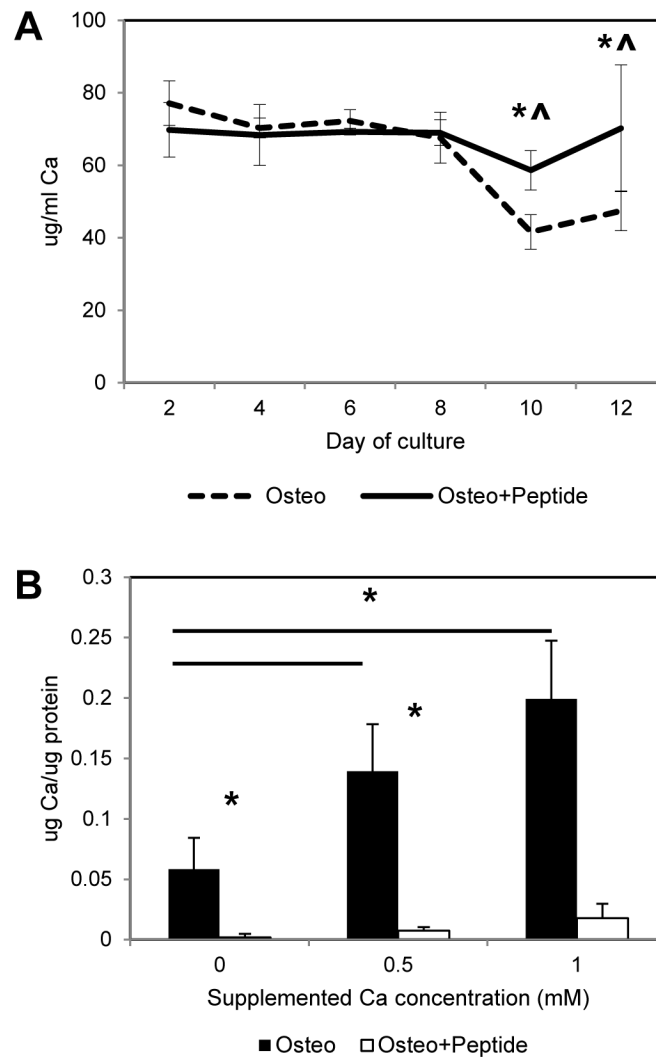


Figure 9.

(A) MC3T3 cells were cultured in osteogenic medium (Osteo) or osteogenic medium supplemented with 300 μ M pVTK peptide (Osteo + Peptide) for 12 days and the media was collected during media changes every 2 days. Quantification of calcium levels in the media showed pVTK treatment resulted in significantly higher calcium levels at days 10 and 12 compared to osteogenic medium controls. [* $p < 0.05$ Osteo vs. Osteo + Peptide at a specific day, t-test, ^ $p < 0.001$ days 2, 4, 6, 8 vs. days 10 and 12 for osteo, 1 way ANOVA on Ranks, Student-Newman-Keuls post hoc test]; (B) MC3T3 cells were cultured in osteogenic medium or osteogenic medium supplemented with 300 μ M pVTK peptide, with or without 0.5 or 1mM of supplemental CaCl_2 for 12 days. Calcium levels (quantified from demineralized cell matrices) were significantly increased with increasing supplemental media calcium levels in osteogenic controls, but no increase in Ca (no mineralization) was seen in peptide treated groups (* $p < 0.05$ compared to groups indicated by bar, or * $p < 0.05$ Osteo vs. Osteo + Peptide at a specific calcium concentration; 1 way ANOVA on Ranks, Student-Newman-Keuls post hoc test within Osteo or Osteo + Peptide treatment across

calcium concentration, t-test between Osteo vs. Osteo + Peptide for a specific calcium concentration)

Author Manuscript

Author Manuscript

Author Manuscript

Author Manuscript

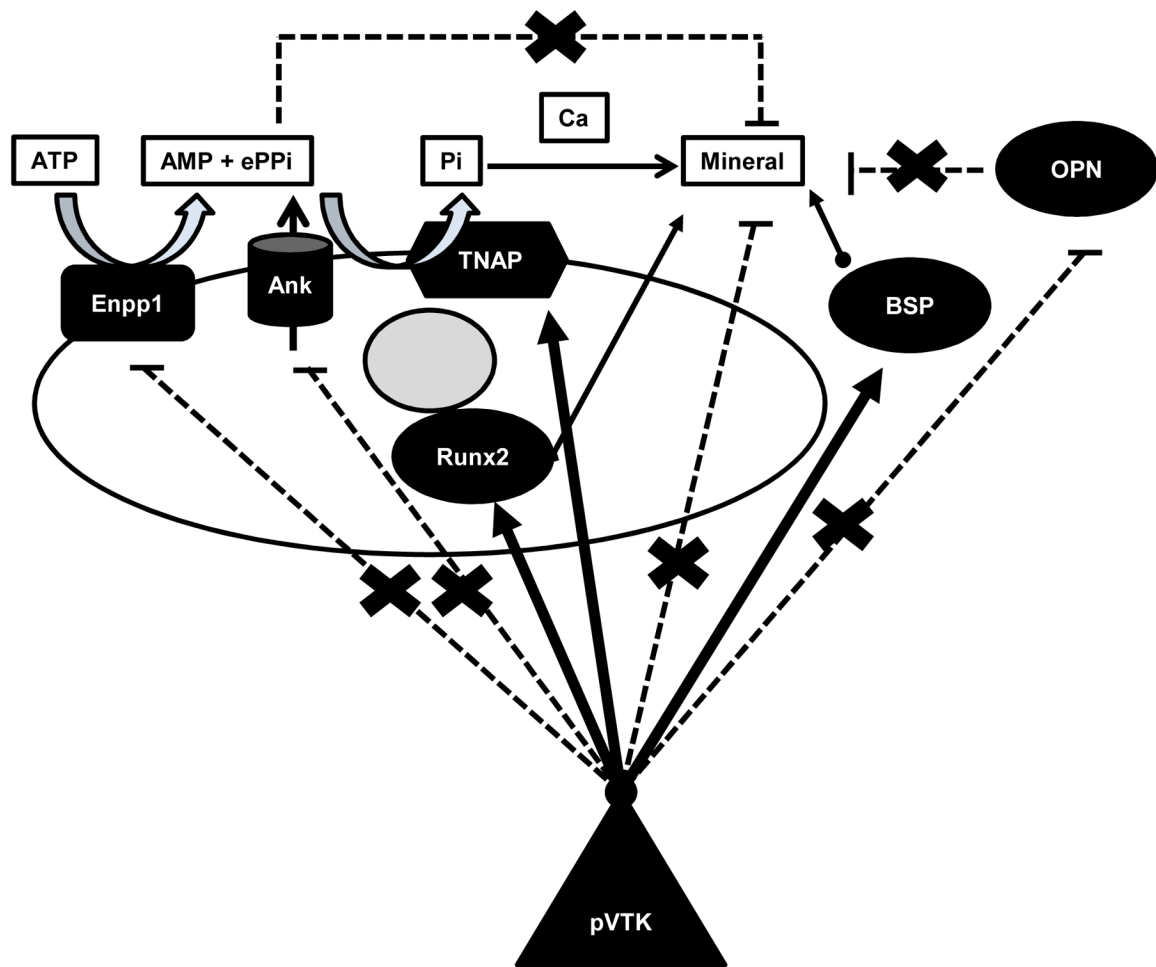


Figure 10.

Schematic summarizing the effect of pVTK on osteoblastic markers. Enpp1, OPN and Ank inhibit mineralization (directly or indirectly via PPi) and were significantly lowered with pVTK administration (dashed lines), whereas TNAP, Runx2 and BSP are positive regulators of mineralization and were significantly increased with pVTK treatment (thick arrows). This data, in concert with the apatite-binding ability of the peptide and temporal sequence of gene expression, suggest a possible compensatory mechanism where the peptide treated cells are attempting to rescue the abnormal mineralization phenotype by downregulating the inhibitors and simultaneously upregulating the promoters.